Electronic Supplementary Material (ESI) for Journal of Materials Chemistry A.

Controllable and Facile One-Pot Synthesis of High Surface Area Amorphous, Crystalline, and Triphasic TiO_2: Catalytic and Photocatalytic Applications

Fatemeh Ariaeinezhad[a], Gholamhossein Mohammadnezhad[a*], Maryam Zare[b], Oluseun Akintola[c], Winfried Plass[c*]

[a] *Department of Chemistry, Isfahan University of Technology, Isfahan, 84156-83111, Islamic Republic of Iran*

[b] *Basic Sciences Group, Golpayegan College of Engineering, Isfahan University of Technology, Golpayegan, Iran.*

[c] *Institut für Anorganische und Analytische Chemie, Friedrich-Schiller-Universität Jena, Humboldtstr. 8, 07743 Jena, Germany.*

[*]Corresponding authors:

Department of Chemistry, Isfahan University of Technology, Isfahan 84156-83111, Islamic Republic of Iran. E-mail: mohammadnezhad@iut.ac.ir, g_m1358@yahoo.com (G. Mohammadnezhad).

Institut für Anorganische und Analytische Chemie, Friedrich-Schiller-Universität Jena, Humboldtstr. 8, 07743 Jena, Germany. E-mail: sekr.plass@uni-jena.de (W. Plass).

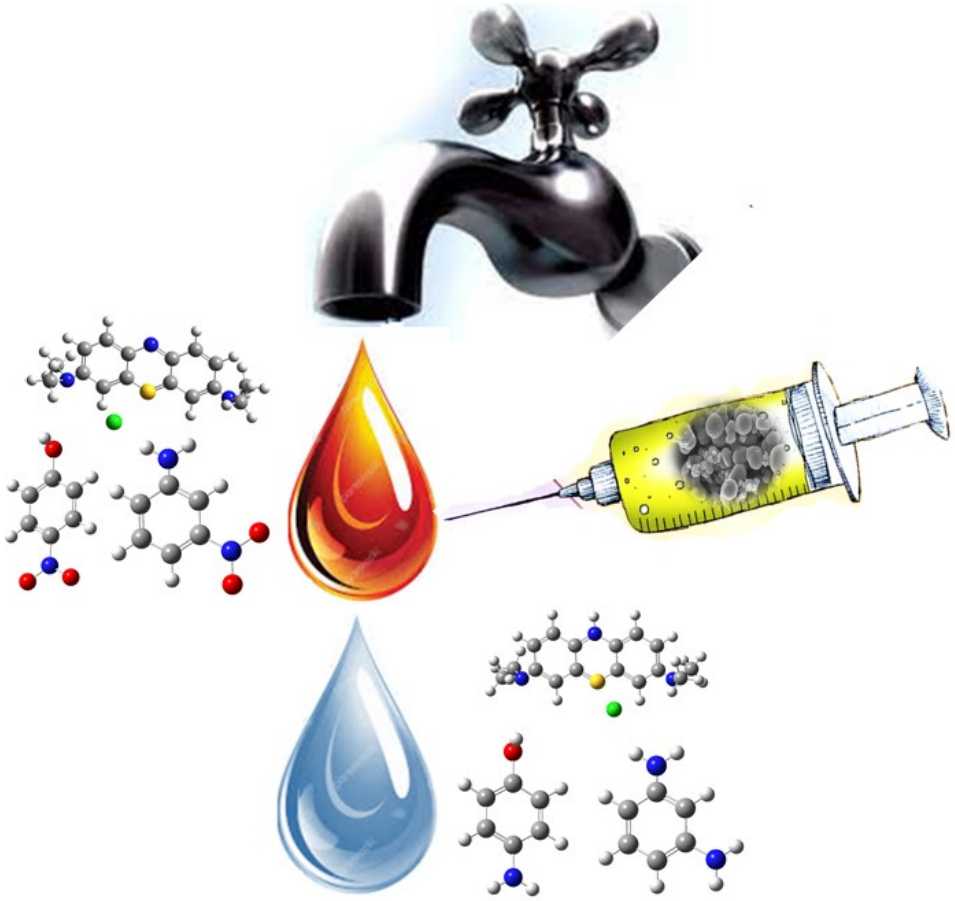

Thermogravimetric Analytical Data

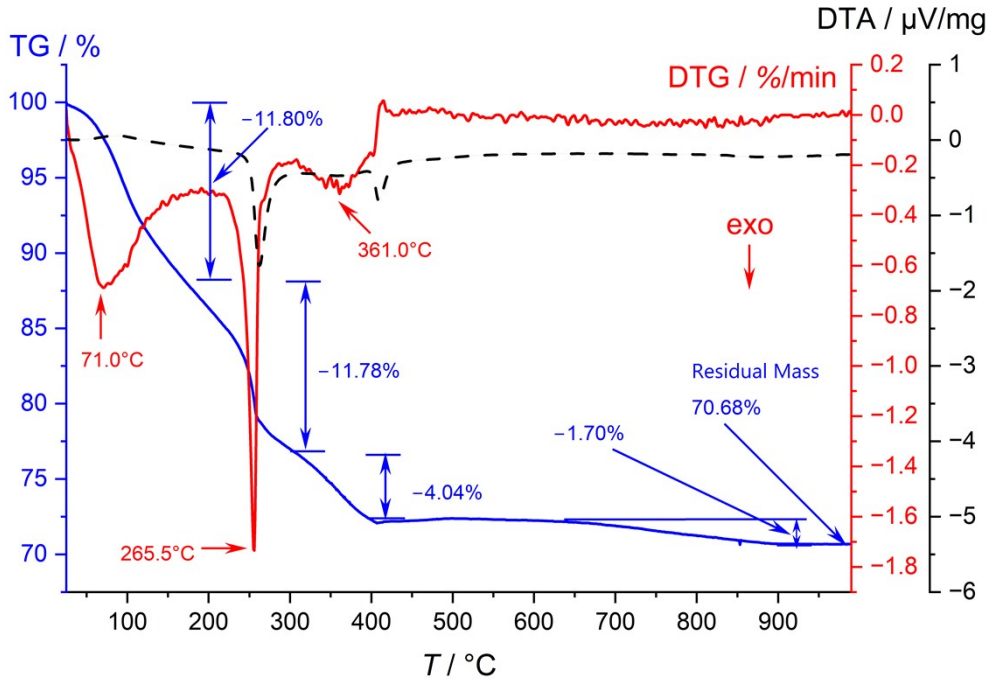

Fig. S1: Thermogravimetric analytical data for Ti-1.

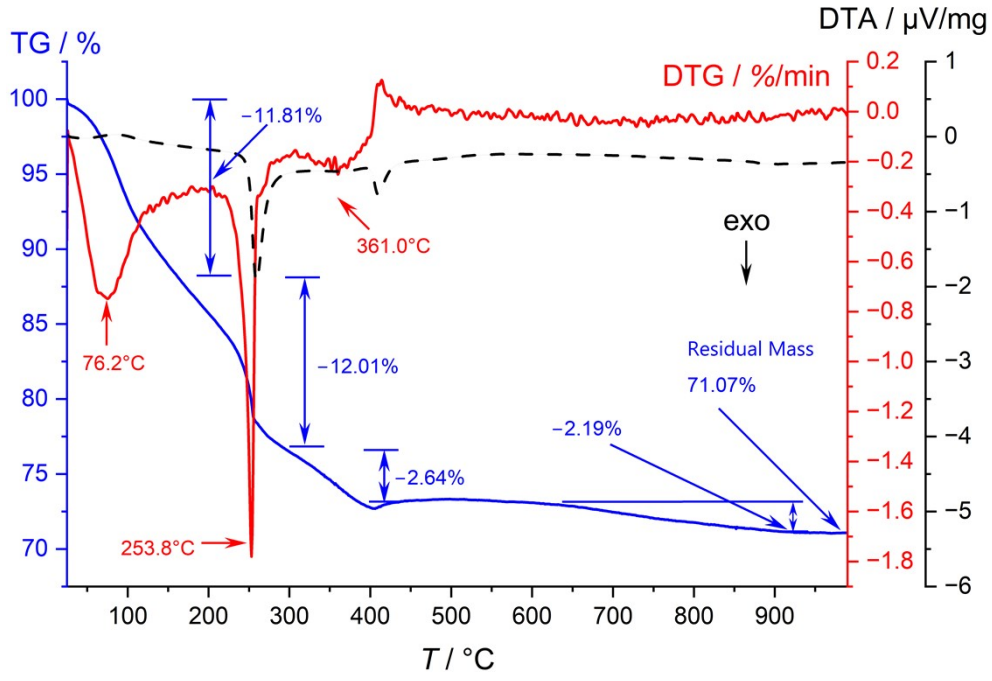

Fig. S2: Thermogravimetric analytical data for Ti-2.

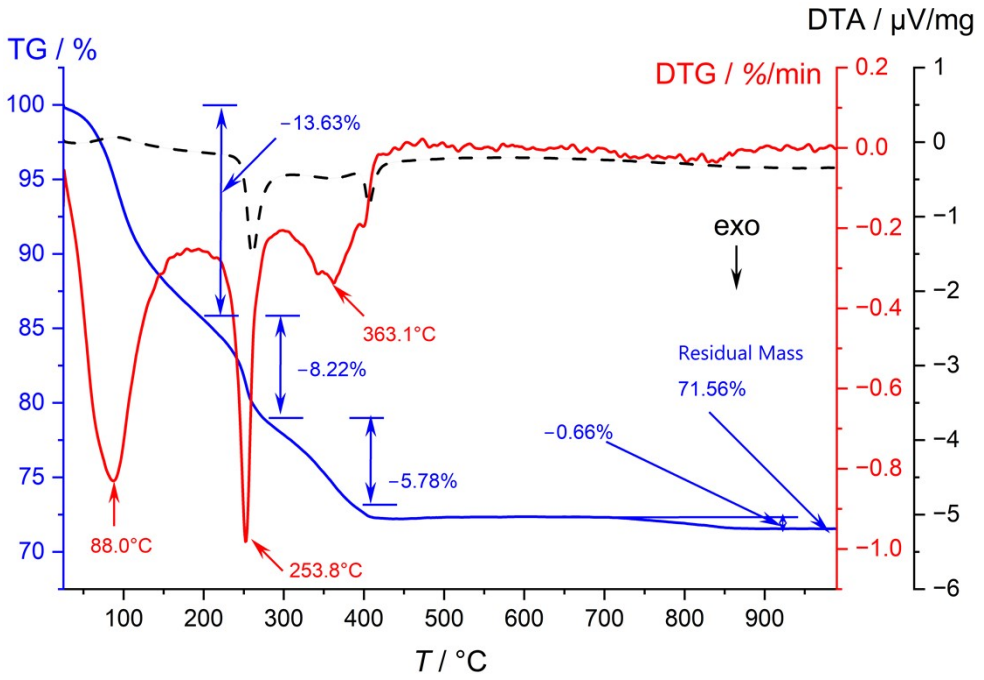

Fig. S3: Thermogravimetric analytical data for Ti-3.

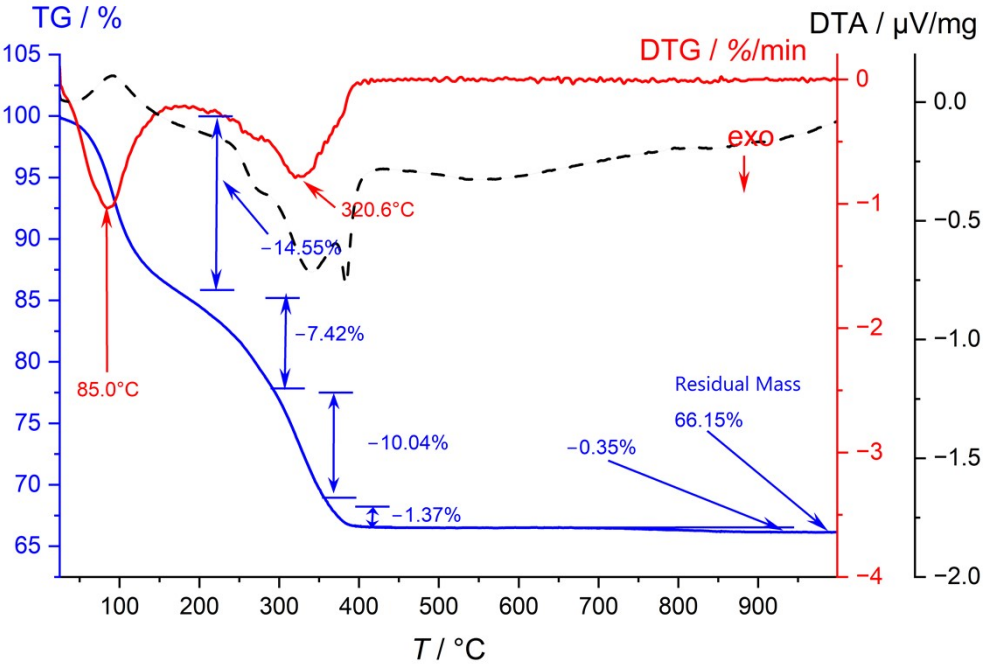

Fig. S4: Thermogravimetric analytical data for Ti-4.

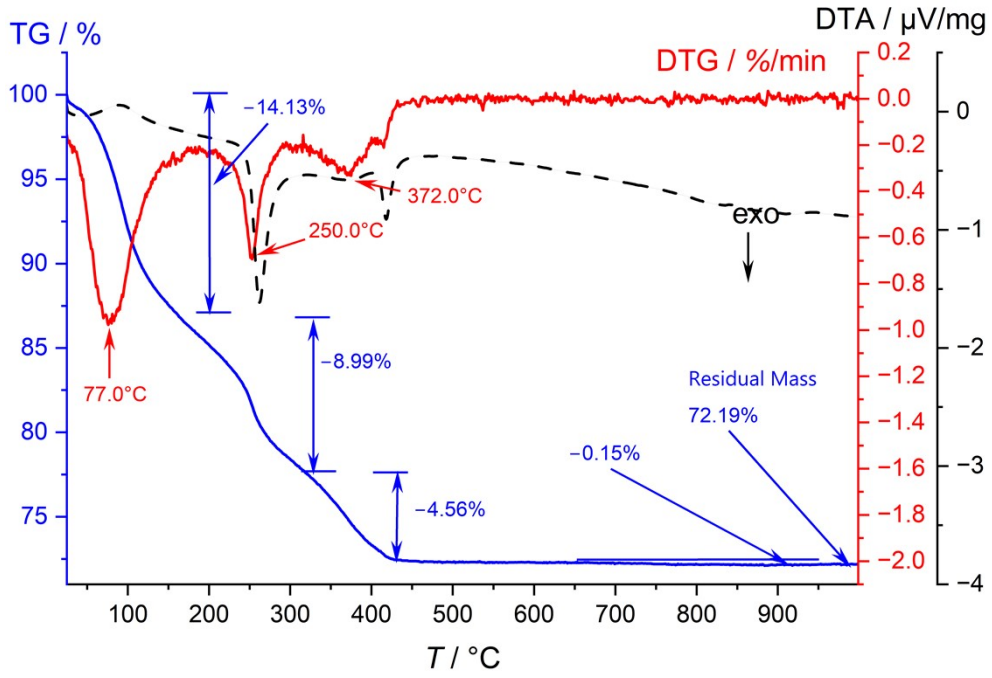

Fig. S5: Thermogravimetric analytical data for Ti-5.

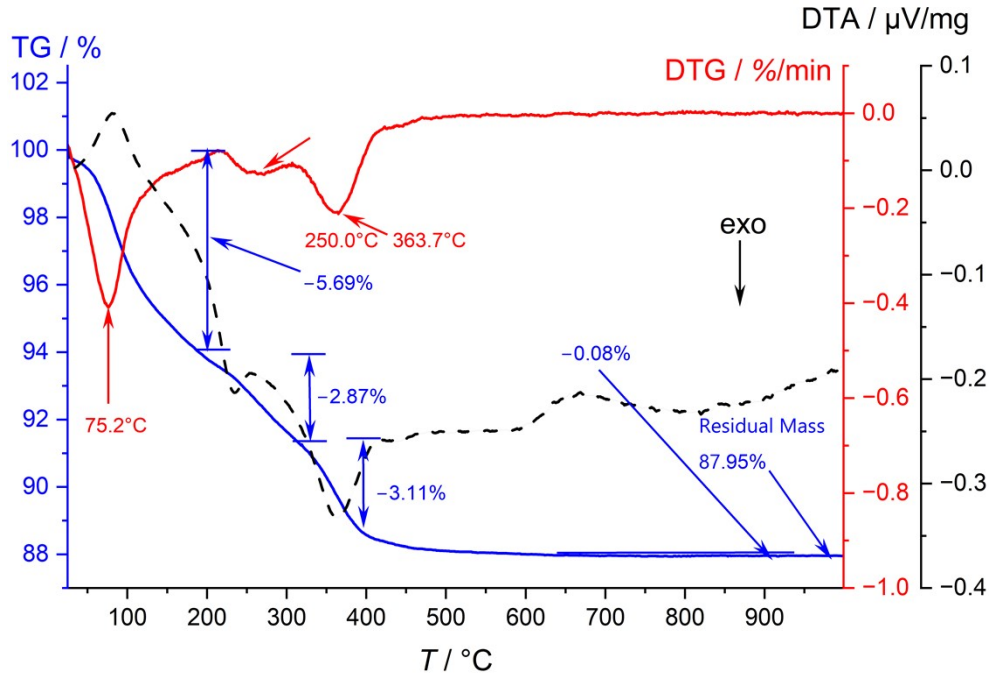

Fig. S6: Thermogravimetric analytical data for Ti-6.

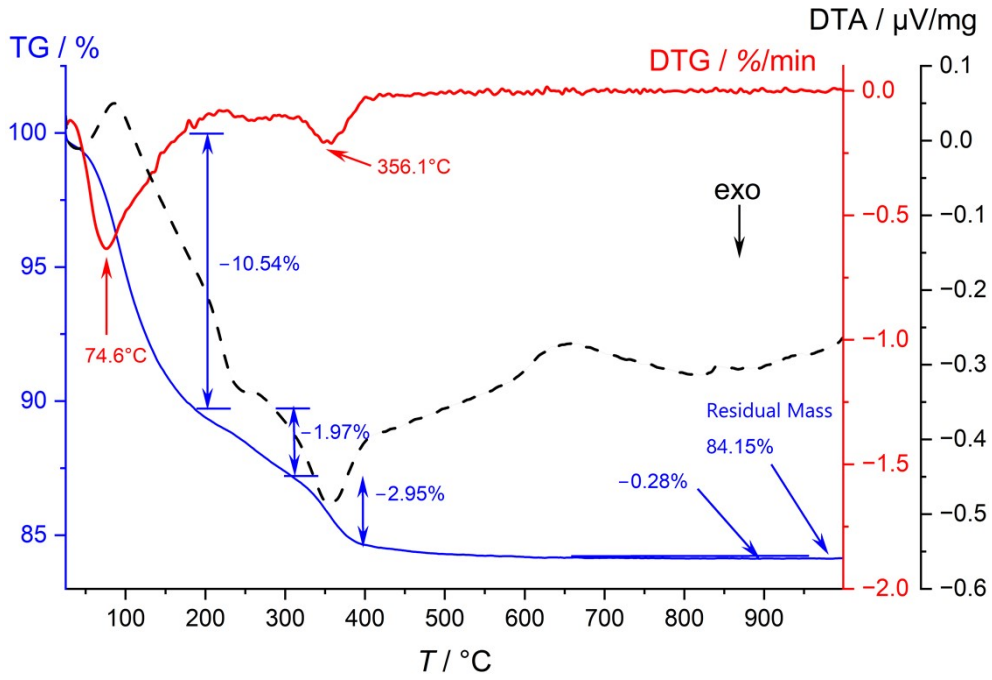

Fig. S7: Thermogravimetric analytical data for Ti-7.

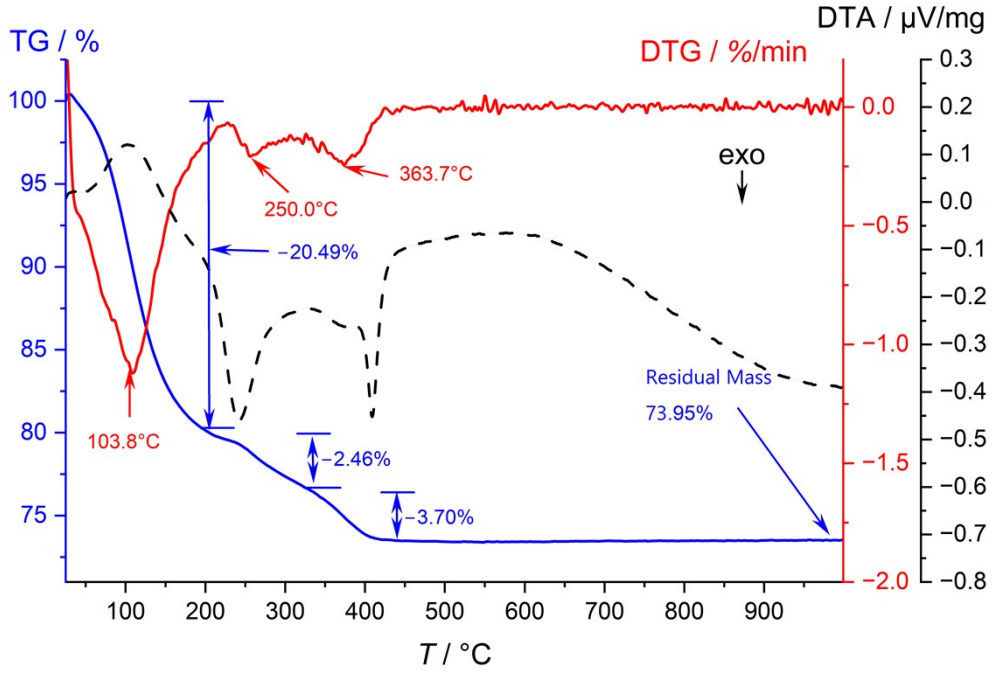

Fig. S8: Thermogravimetric analytical data for Ti-8.

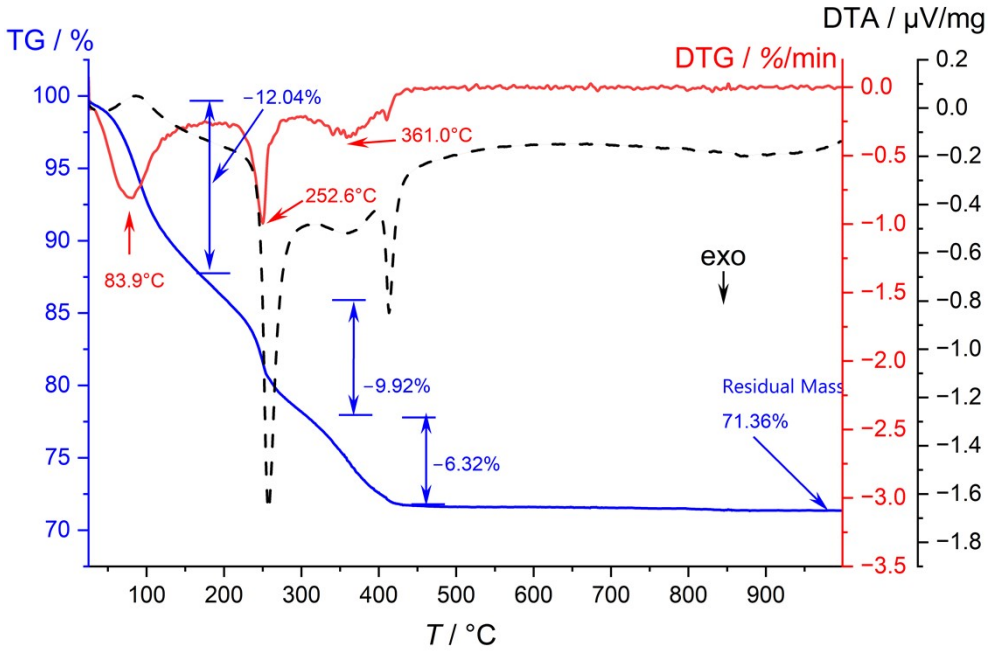

Fig. S9: Thermogravimetric analytical data for Ti-9.

Comparison of reagent ratio and porous properties of nanoparticles

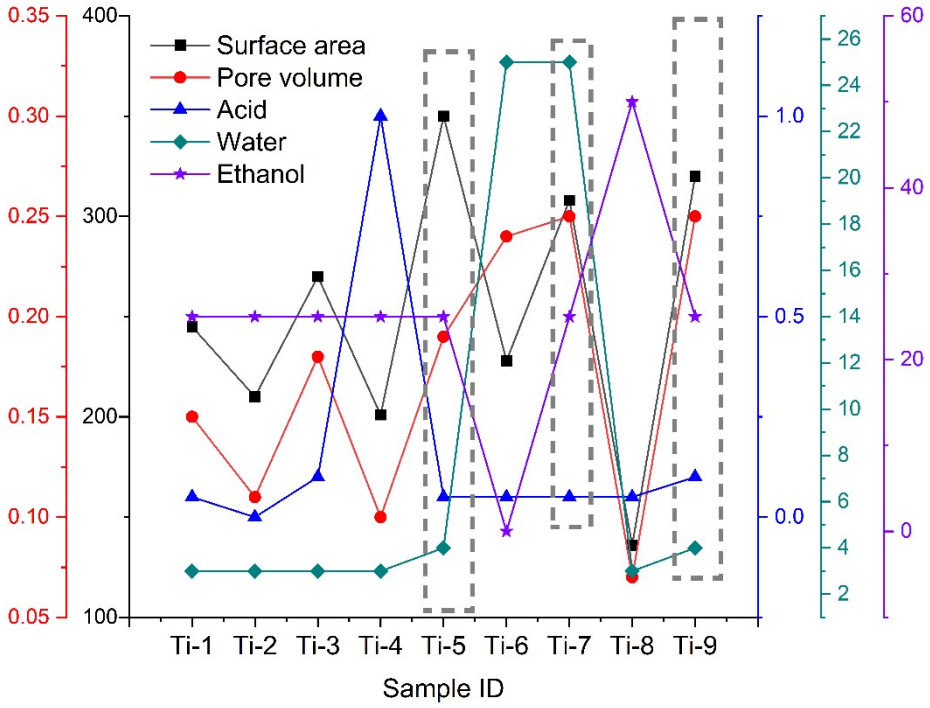

Fig. S10: Comparison of the quantity of reagents used in hydrolyses of TiO_2 nanoparticles with porous properties. Dashed rectangles serve to highlight best performing nanoparticles with regard to their pore volumes and surface areas as well as the relative quantity of individual reagents used during their hydrolyses.

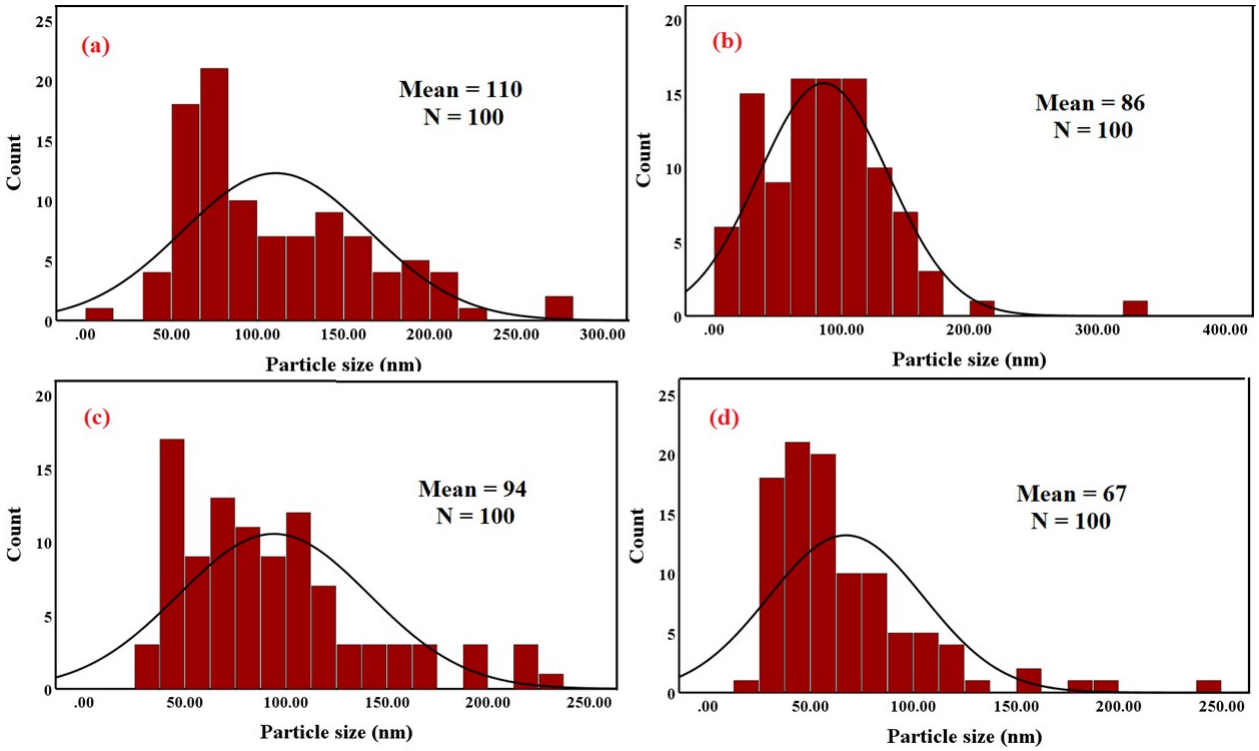

Fig. S11 Histogram curves of TiO_2 Nanoparticles (Ti-3 (a), Ti-5 (b), Ti-7 (c) and Ti-9 (d)).

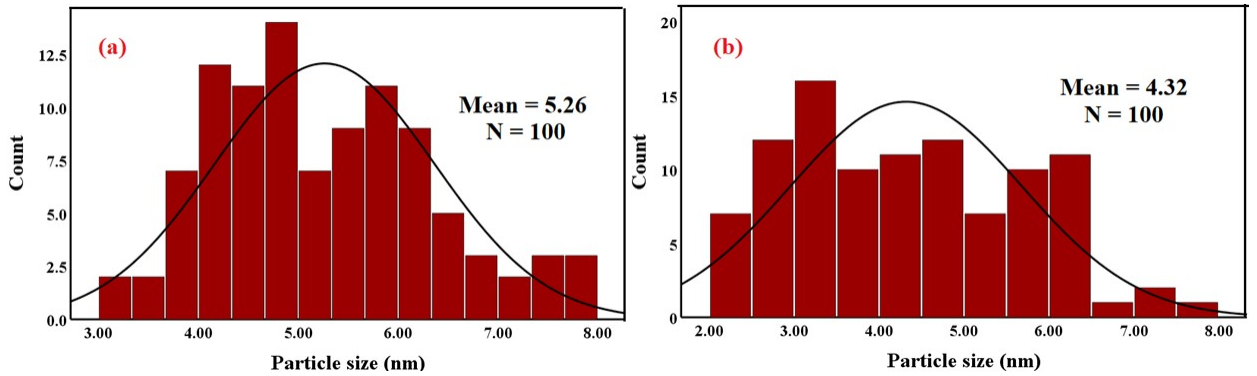

Fig. S12 Histogram curves of TiO_2 Nanoparticles (Ti-6 (a) and Ti-7 (b)).

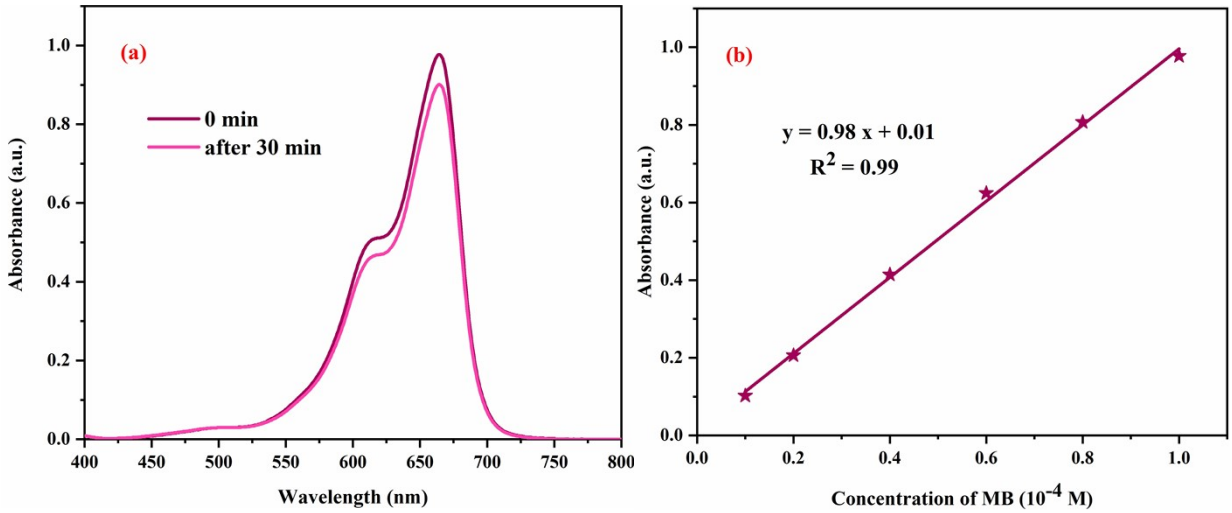

Fig. S13 (a) UV–visible absorption spectra for the photodegradation of MB dye solution under darkness in the presence of H_2O_2 with Ti-9, and (b) the calibration curve in different concentrations.

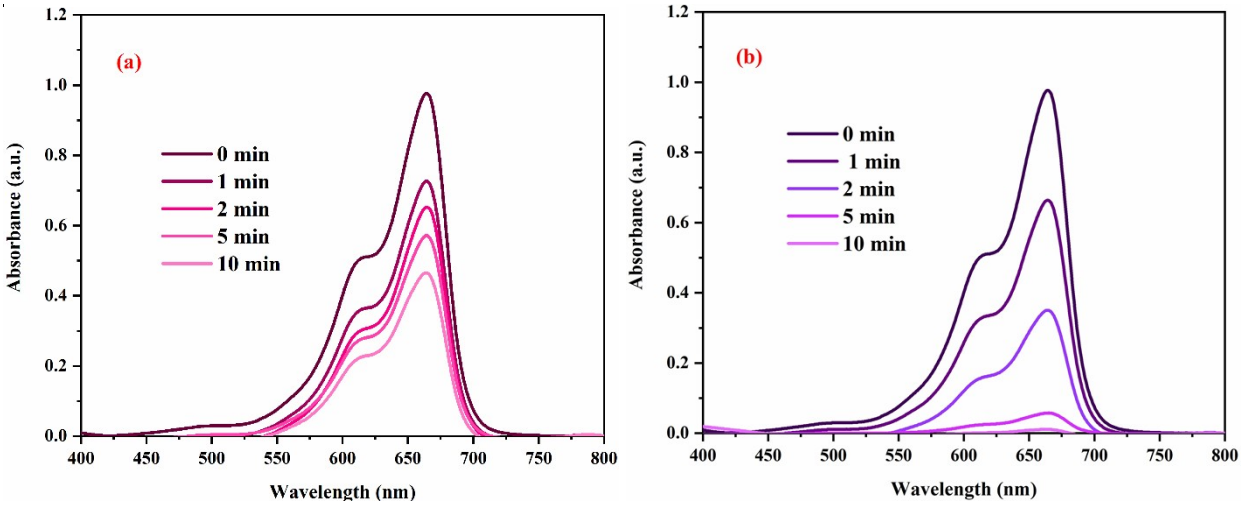

Fig. S14 Time-dependent UV–visible absorption spectra for the photodegradation of MB dye solution under visible light in the presence of H_2O_2 (a), with 5 mg of Ti-9, and (b) with 15 mg of Ti-9.

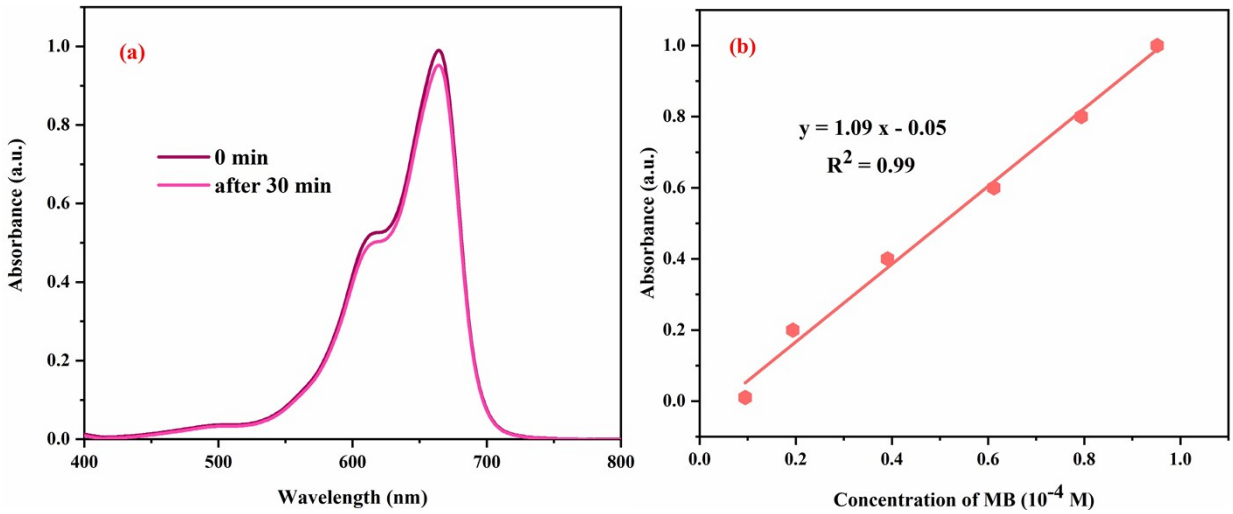

Fig. S15 Time-dependent UV–visible absorption spectra for the reduction of MB in the presence of $NaBH_4$ (a) in the absence of Ti-9, and (b) its calibration curve in different concentrations.

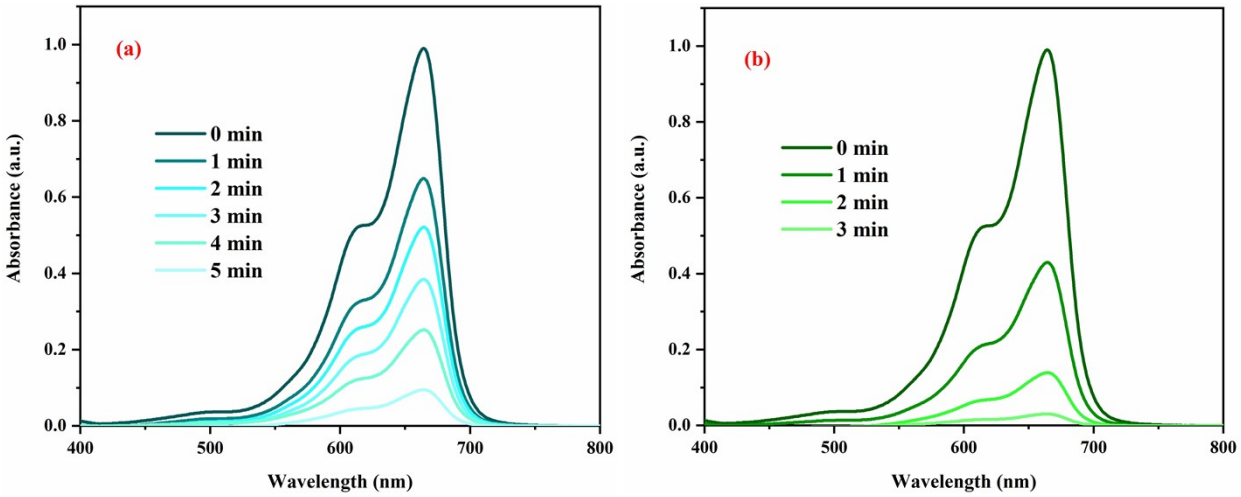

Fig. S16 Time-dependent UV–visible absorption spectra for the reduction of MB in the presence of $NaBH_4$ (a) with 5 mg of Ti-9, and (b) with 15 mg of Ti-9.

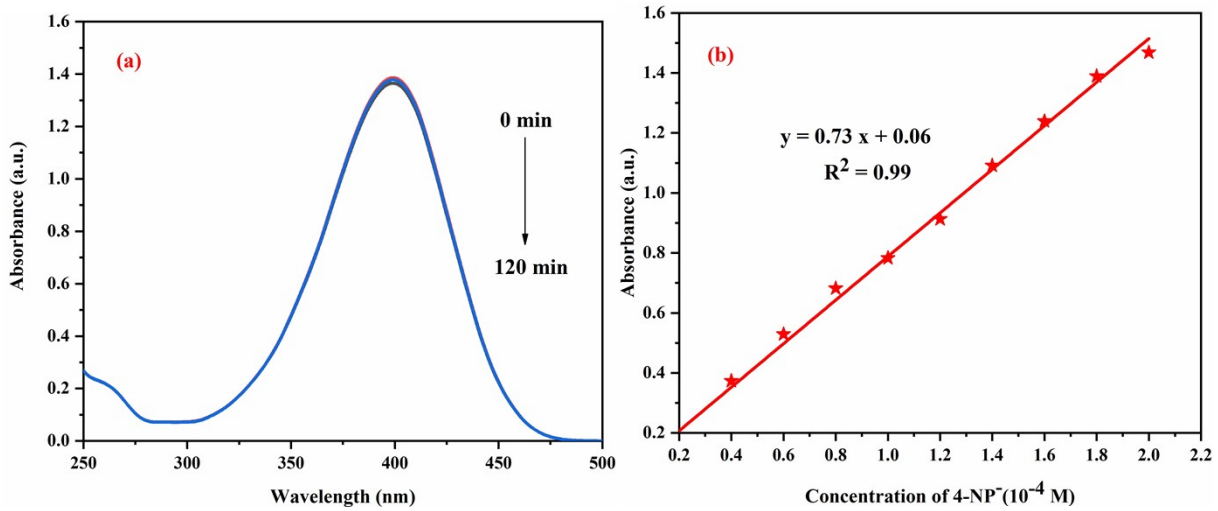

Fig. S17 Time-dependent UV–visible absorption spectra for the reduction of 4-NP with $NaBH_4$ (a) in the absence of Ti-9 (b) the calibration curve of 4-nitrophenolate ($4\text{-}NP^-$) intermediate in the absence of the Ti-9.

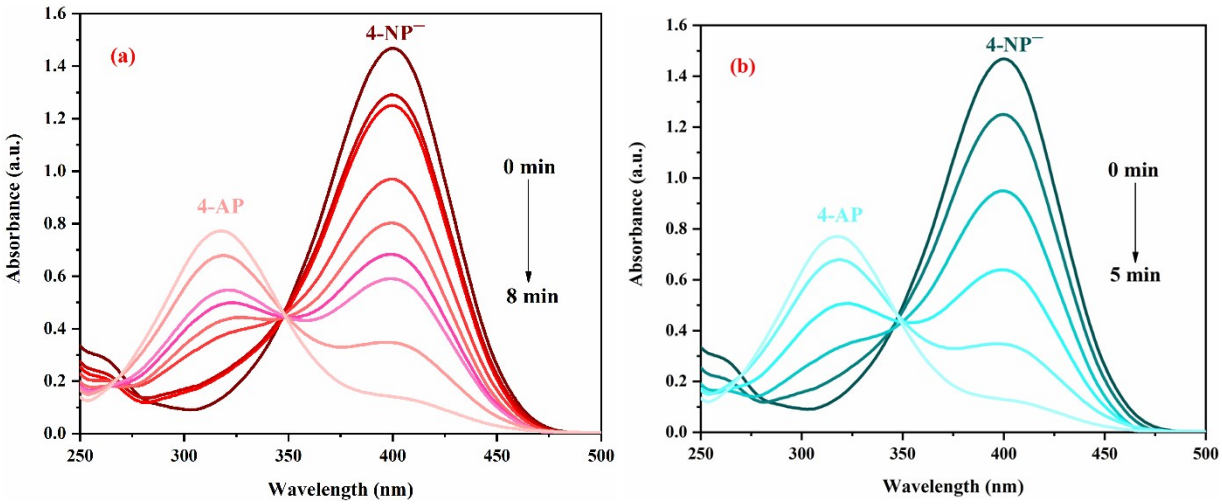

Fig. S18 Time-dependent UV–visible absorption spectra for the reduction of 4-NP in the presence of $NaBH_4$ (a) with 1 mg Ti-9, and (b) with 3 mg Ti-9.

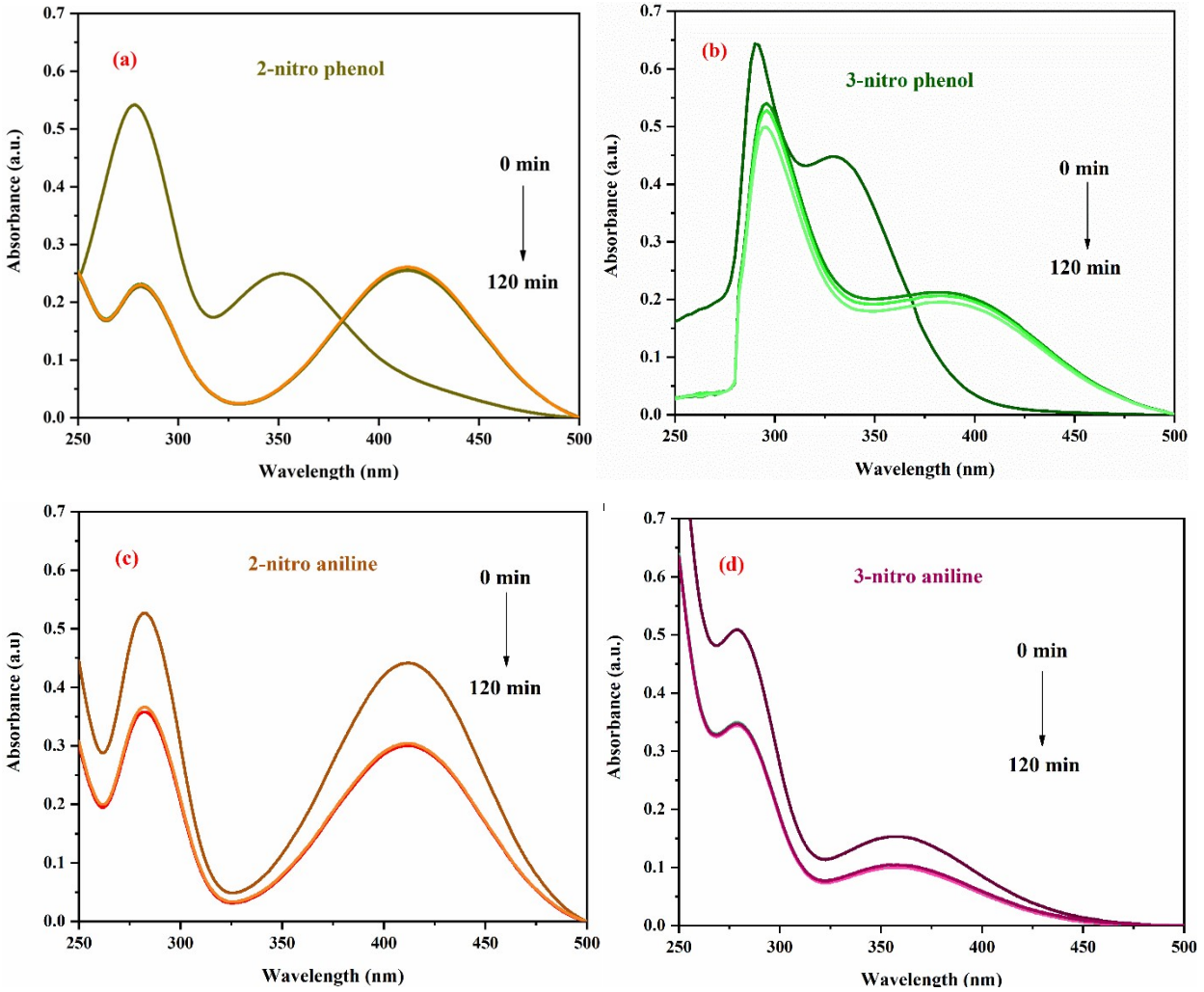

Fig. S19 Time-dependent UV–visible absorption spectra for the reduction of (a) 2-NP, (b) 3-NP, (c) 2-NA, and (d) 3-NA, all with $NaBH_4$ in the absence of the Ti-9.

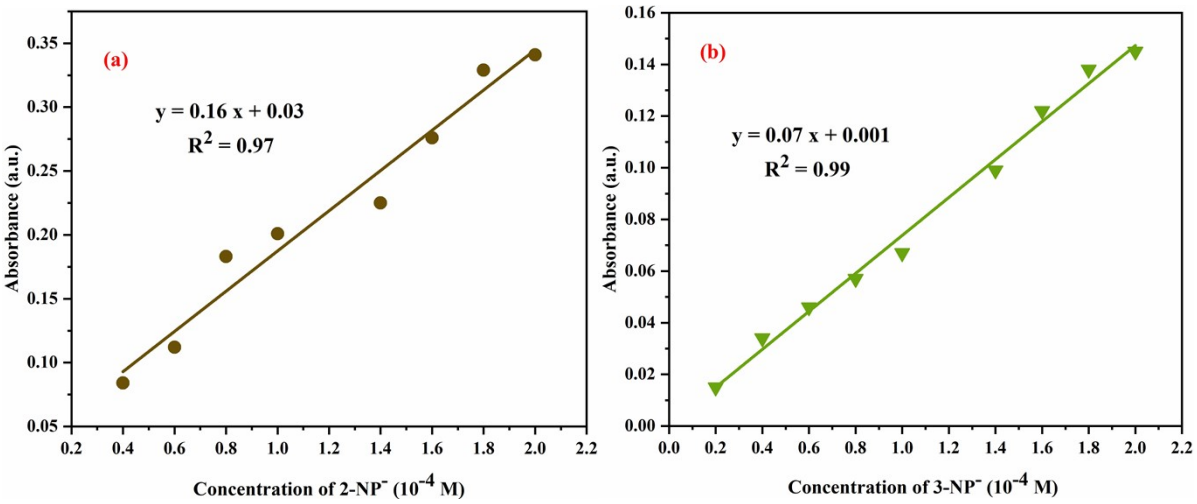

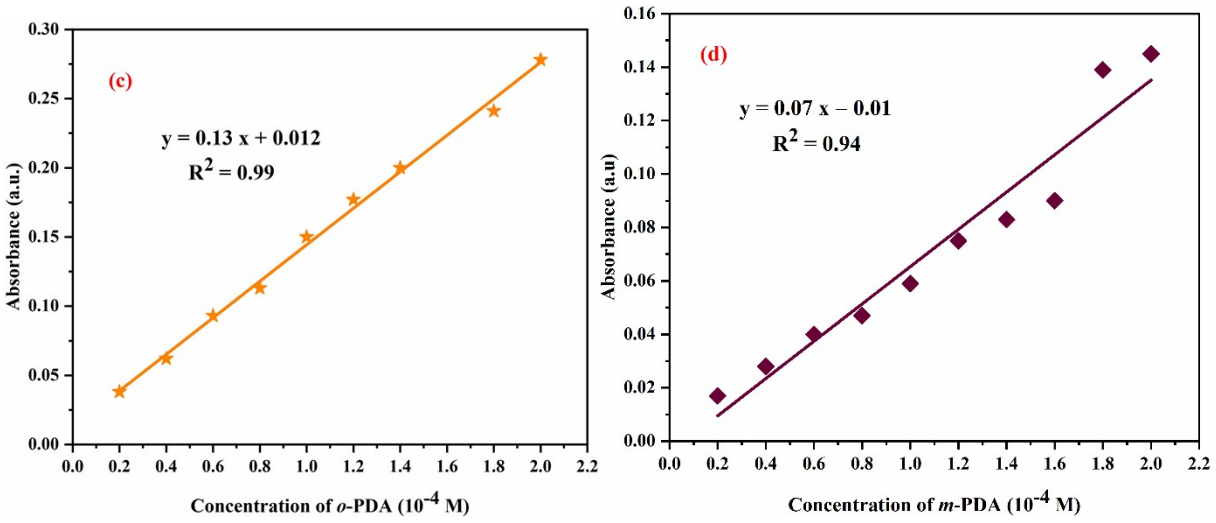

Fig. S20 Calibration curves of intermediates (a) 2-NP$^-$, (b) 3-NP$^-$, (c) *o*-PDA, and (d) *m*-PDA, all with $NaBH_4$ in the absence of the Ti-9.

Tab. S1: A summary of consistency parameters derived from fitting isotherms to

	Ti-1	**Ti-2**	**Ti-3**	**Ti-4**	**Ti-5**	**Ti-6**	**Ti-7**	**Ti-8**	**Ti-9**
P/P_0 *range*	0.007–0.102	0.007–0.103	0.010–0.152	0.007–0.101	0.009–0.126	0.125–0.276	0.149–0.300	0.005–0.078	0.025–0.127
C	325.07	344.465	202.206	292.235	175.323	22.515	15.030	693.685	132.855
V_m (cm^3/g)	64.3	55.2	70.5	52.6	93.7	59.7	80.6	35.6	83.99
$1/\sqrt{C}+1$	0.053	0.051	0.065	0.055	0.070	0.174	0.205	0.038	0.079
$P/P_0(V_m)$	0.054	0.051	0.065	0.058	0.073	0.175	0.206	0.039	0.079
*a*BET (m^2/g)	245	210	270	200	350	230	310	140	320
R	0.9999	0.9999	0.9999	0.9999	0.9999	0.9999	0.9998	0.9999	0.9999